

# Analyst

Accepted Manuscript



This is an *Accepted Manuscript*, which has been through the Royal Society of Chemistry peer review process and has been accepted for publication.

*Accepted Manuscripts* are published online shortly after acceptance, before technical editing, formatting and proof reading. Using this free service, authors can make their results available to the community, in citable form, before we publish the edited article. We will replace this *Accepted Manuscript* with the edited and formatted *Advance Article* as soon as it is available.

You can find more information about *Accepted Manuscripts* in the [Information for Authors](#).

Please note that technical editing may introduce minor changes to the text and/or graphics, which may alter content. The journal's standard [Terms & Conditions](#) and the [Ethical guidelines](#) still apply. In no event shall the Royal Society of Chemistry be held responsible for any errors or omissions in this *Accepted Manuscript* or any consequences arising from the use of any information it contains.



Analyst

ARTICLE

## Optical microscopic imaging diagnosis of the pharmacological reaction of mouse embryonic stem cell-derived cardiomyocytes (mESC-CMs)

Received 00th January 20xx,  
Accepted 00th January 20xx

DOI: 10.1039/x0xx00000x

www.rsc.org/

Tomohiko Ikeuchi,<sup>a</sup> Wilfred Espulgar,<sup>a\*</sup> Eiichi Shimizu,<sup>a</sup> Masato Saito,<sup>a</sup> Jong-Kook Lee,<sup>b</sup> Xiaoming Dou,<sup>c</sup> Yoshinori Yamaguchi,<sup>ac</sup> Eiichi Tamiya<sup>ad\*</sup>

Quantitative diagnosis of pharmacological chronotropic reactions on mouse embryonic stem cell-derived cardiomyocytes (mESC-CMs) was successfully performed by utilizing derivative imaging analysis on videos recorded with a microscope camera at 30 Hz frame rate and 680×510 pixel resolution. The imaging analysis algorithm, developed in our lab, generated the contractile profile of the cells which was exploited for drug effect profiling. Six drugs such as isoproterenol (0.01–1 μM), quinidine (2–200 μM), propranolol (0.03–30 μM), verapamil (0.01–1 μM), sotalol (1–100 μM), and acetylsalicylic acid (1–10 μM) were administered and the quantitative medication effect was determined. Among the negative chronotropic agents administered, verapamil was found to be the most potent while sotalol was found to be the least potent in the micromolar level. Simultaneous measurement of the field potential and contractile motion in the verapamil effect test showed a coherent result. Moreover, this approach can provide insights about the contraction-relaxation condition which is not available in the common electrophysiological approach. With these findings, it is expected that this study can aid in providing a simple and reliable *in vitro* mESC-CM-based screening platform for cardiovascular effect profiling of candidate drugs.

### Introduction

Cell-based drug assay is a common technology among pharmaceutical companies for rapidly screening chemical entities during initial discovery phase and for mechanistic detailed studies during developmental phase.<sup>1</sup> The candidate drug compound is administered on trans-genetic cell lines and then the cell's response is diagnosed. Among the screening processes, cardiovascular toxicity profiling of chemical entities proved to be the greatest obstacle. Majority of the withdrawal of the registered drugs in the market is found to be brought by the unexpected cardiovascular events when administered for a longer duration and to a bigger population.<sup>2–4</sup>

For decades, cardiomyocyte (CM) cells have been utilized in cell-based drug screening and profiling for cardiovascular effects of drug candidates.<sup>5–8</sup> There are two cell types utilized in CM-based drug screening. The primary cultured CMs and

the stem cell derived CMs. The primary cultured CMs are prepared from sacrificed mouse or other animals that are phylogenetically close to humans. Cell-based assay that uses primary cultured human CMs are expensive, has time-consuming mass production, and can pose ethical issues. The ES derived- and iPS derived-CM are more ideal for cell-based drug assay system because of its infinite proliferation and genetic potential.<sup>6,8–13</sup>

In a CM-based drug testing, quantification of beat rate has been commonly utilized in understanding the physiological behaviour in response to drug administration. Significant change in the beat rate is a pathognomonic sign. Several tools had been used in beat rate quantification of the cells by measuring the membrane potential,<sup>14–18</sup> Ca<sup>2+</sup> concentration,<sup>19–21</sup> and physical movement of the cell.<sup>22–30</sup>

In cardiac electrophysiology, patch clamp<sup>14,15</sup> and multi-electrode array (MEA)<sup>16–18</sup> technologies have been employed to measure the action potential and count the beat occurrences. The action potential is an electric signal that corresponds with the contraction-relaxation motion of the cell. The measurement of the action potential provides information on the timing of the beat initiation and the ion transmission through the cell membrane. Patch clamp requires sticking the electrode directly to the target cells which requires adept technical skill to perform and is also labour intensive. For MEA, it measures the field potential around a group of cells which is directly correlated with the action potential. The average potential around the cell is measured that varies depending on

<sup>a</sup> Department of Applied Physics, Graduate School of Engineering, Osaka University, 2-1, Yamadaoka, Suita, Osaka, 565-0871, Japan. E-mail: wilfred@ap.eng.osaka-u.ac.jp; tamiya@ap.eng.osaka-u.ac.jp

<sup>b</sup> Department of Cardiovascular Regenerative Medicine, Osaka University, 2-1 Yamadaoka, Suita, Osaka, 565-0871, Japan.

<sup>c</sup> Photonics and Bio-medical Research Institute, Department of Physics, Faculty of Science, East China University of Science and Technology (ECUST), Shanghai, China.

<sup>d</sup> Photonics Advanced Research Center (PARC), Graduate School of Engineering, Osaka University, 2-1, Yamadaoka, Suita, Osaka, 565-0871, Japan. E-mail: tamiya@ap.eng.osaka-u.ac.jp

the separation distance of the target to the electrode probe. In both methods, direct physical contact is required to measure the beat rate which limits its functionality.

Calcium ions can be monitored and measured by a  $\text{Ca}^{2+}$  sensitive fluorescent dye. The beat rate is derived from the change in fluorescence intensities inside the cell.<sup>19,20</sup> This is made possible because  $\text{Ca}^{2+}$  flux corresponds to the contraction of the CMs. However, the use of fluorescent dye is hampered by its phototoxicity which can damage the cells and degrade the signal quality.<sup>21</sup> In addition, the use of an external agent aside from the drug of interest might provide a biased or false profile.

Other methods such as Scanning Ion Conductance Microscopy (SICM)<sup>22,23</sup> and Light Addressable Potentiometric Sensor (LAPS)<sup>24</sup> utilize topographic differences between contraction and relaxation motion to quantify the beat rate. SICM is based on the working principle of scanning-tunnelling microscopy but combined with patch clamp. The probe detects the difference of ion conductance outside the CMs and the topography can be generated and displayed on the screen. This technique has realized the arbitrary measurement in any place of the cardiomyocyte cell by simply moving the probe. However, like scanning-tunnelling microscopy, advanced operational skill is required. LAPS, on the other hand, utilizes a photosensitive semiconductor. CMs are grown on the substrate and illuminated by LEDs. The contraction of the cells alters the optical path of the light and, in effect, the fluctuations will be reflected in the photocurrent measured. However, since the substrate is opaque, other studies like optical imaging to determine the physiological condition of the cell is limited.

In this study, video microscopy has been utilized to investigate the contractile motion of the cells that was used to quantitatively diagnose the chronotropic effect of the selected drugs. Optical microscopic diagnosis is a non-invasive and versatile tool for analysing biological samples. Simultaneous measurement with MEA is feasible which can provide better insights on the drug pathway framework. The contractile profile of the mouse stem cell-derived cardiomyocytes (mESC-CMs) used in this study was generated from the derivative image analysis as previously reported.<sup>31</sup> This imaging analysis has also been reported applicable in generating the beat profile of a single primary cultured neonatal rat CM<sup>32</sup> with high signal to noise ratio and, thus, not requiring any noise filtration algorithm. In comparison to other label-free video microscopy approaches that use edge-detection method<sup>18,25,27</sup> and image correlation analysis,<sup>28–30</sup> this approach is not limited by the need for an expensive high speed camera and a higher resolution. Thus, this is expected to have lower system requirement for processing and storage; more accessible and applicable to major users. With these, it is expected that this tool can greatly help the pharmaceutical industry for pharmacological profiling of the cardiovascular effect in drug development.

## Materials and Methods

### Cell culture and differentiation into cardiomyocyte

Fig. 1a illustrates the culture and plating stages of the cells for drug effect test. Mouse ES cells (mESCs) B6G2 (Riken cell bank, Ibaraki, Japan) were cultured at 37 °C in an atmosphere of 5%  $\text{CO}_2$  on mitomycin C treated STO (ECACC, Salisbury, UK) feeder layer in culture medium. The culture medium consisted of DMEM high glucose (Nacalai Tesque, Inc., Kyoto, Japan), supplemented with 15% FBS (Gibco, Life Technologies, CA, USA), 0.1 mM non-essential amino acids, 2 mM L-glutamine, 50 U/mL penicillin and 50  $\mu\text{g}/\text{mL}$  streptomycin, 0.1  $\mu\text{M}$   $\beta$ -mercaptoethanol; purchased from Invitrogen (Life Technologies, CA, USA), and 1000 U/mL recombinant Leukaemia inhibitory factor (LIF, Chemicon, Merck Millipore, Darmstadt, Germany). STO cells (ECACC) were grown at 37 °C in an atmosphere of 5%  $\text{CO}_2$ . For STO cell culture, the medium containing DMEM high glucose supplemented with 10% FBS, 2 mM L-glutamine, 50 U/mL penicillin and 50  $\mu\text{g}/\text{mL}$  streptomycin were used. As they reached confluent stage, STO cells were exposed to 10  $\mu\text{g}/\text{mL}$  mitomycin C (Wako, Osaka, Japan) for 2.15 h. The mitomycin C-treated STO cells were washed in PBS and plated in gelatine-coated tissue culture dishes to form the feeder layer and incubated overnight before plating the ES cells on a separate dish.

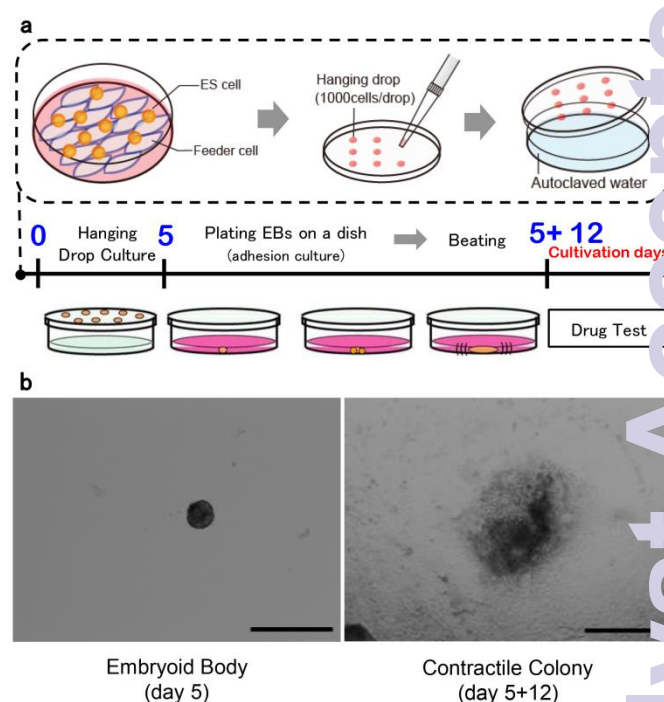


**Fig. 1.** The mESC differentiation into cardiac myocytes. (a) The time scale of the preparation and culture for drug test. Hanging drop method was utilized to prepare EBs. (b) The growth of tissue from (left panel) day 5 as EB to (right panel) contractile colony at day 5+12 on a 0.1% gelatine-coated petri dish. (Scale bar = 500  $\mu\text{m}$ )

After 2 days, cells were treated with trypsin (0.05% Trypsin-EDTA, Invitrogen, Life Technologies, CA, USA) to prepare single mES cell suspension and then the number of

## Analyst

cells was counted. To induce differentiation, cells were cultivated into cellular clusters called embryoid body (EB) by hanging drop method, where 1000 cells were cultured in each drop of 20  $\mu\text{L}$  differentiation medium; components similar to mESC cell medium without LIF. The drops were put on the inner side of the lid of a 100 mm culture dish (Iwaki, Tokyo, Japan) and the bottom of the dish was filled with an autoclaved Milli-Q water to avoid medium dehydration. The cells were cultured under 5%  $\text{CO}_2$  at 37  $^\circ\text{C}$  for 5 days by hanging drop method until it grew to EB cells. The sizes ranged from 100  $\mu\text{m}$  and 500  $\mu\text{m}$ .

EBs (Fig. 1b left panel) were transferred to 0.1% gelatine-coated 10 mm culture dish filled with 10 mL of differentiation medium and then cultured at 37  $^\circ\text{C}$  in an atmosphere of 5%  $\text{CO}_2$ . Medium replacement was done every day. The EBs were cultured until they differentiated to stable contracting cardiomyocytes;  $\sim 12$  days after transferring and plating (Fig. 1B right panel).

### Digital movie recording system

The EBs were observed under an inverted microscope (IX71, Olympus, Tokyo, Japan) equipped with a digital colour CCD camera (DP71, Olympus, Tokyo, Japan). During video recording, the petri dish containing the cells was set on a thermal plate (TOKAI HIT, Shizuoka, Japan) heated at 37  $^\circ\text{C}$ . The video was recorded with a 4X objective lens at 30 fps in binning mode and 680 $\times$ 510 pixel resolution with 8-bit depth format as sequential bright field images. Imaging analysis was performed by an imaging quantitative algorithm developed at our lab.<sup>31</sup>

### Quantitative imaging analysis

Inter-beat duration and, subsequently, beat rate were quantified based on the total pixel intensity variation in the digital movie recording of the beat motion as previously described.<sup>31</sup> Briefly, movie recordings of the beating colonies were converted into sequential frames and the pixel intensities of each resulting frame were normalized. Quantitative intensity was obtained by calculating the total pixel intensity of the pixel intensity difference of the frames in succession. Fig. 2a shows an example of the resulting beat profile. The interval between successive peaks were computed and converted into histograms which were then Gaussian fit to obtain the mean beat interval (Fig. 2b). Based on this method, the change ratio of beat interval is defined for pharmacological responses of mESC-CMs as:

$$\text{change ratio (\%)} = 100 \times \frac{(a-b)}{a} \quad (1)$$

where  $a$  is the beat interval before administration and  $b$  is the beat interval after administration. A positive change ratio indicates an increase in beat rate and a decrease in beat interval while a negative change ratio indicates a decrease in beat rate and an increase in beat interval.

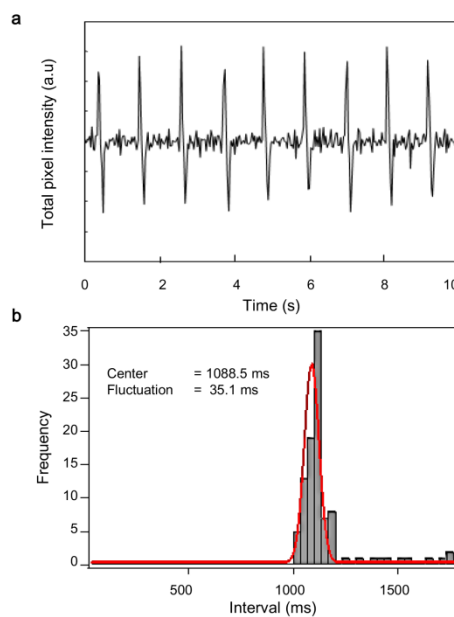


Fig. 2. Sample scheme of beat profile generation and beat interval quantification. (a) Time domain of the pixel intensity variation of the derivative images produced. The positive amplitude represents the systolic or contraction phase while the negative amplitude represents the diastolic or relaxation phase. (b) Histogram of the beat intervals that was measured from the previous graph. After Gaussian fitting, the mean beat interval was deduced.

### Drug loading test

After 12 days of culturing, drug test was performed by comparing the contractile behaviour of the cell before and after drug administration. The beat behaviour of the mESC-CMs in 5 mL culture medium without drug was first recorded for 2 min. Contractile colonies with beat interval ranging from 600 ms (100 bpm) to 2500 ms (24 bpm) were selected for drug effect test. Five millilitres of the drug solution was then carefully added and mixed to the culture resulting to the desired molar concentration. After 1 min, the beat behaviour of the same colonies was recorded for 2 min. To bring the cells back to the original state, the old medium was aspirated and the cells were washed with fresh medium twice and then placed in the incubator for 10 min. The same cells were subjected to the same drug with different concentration and observed in the similar way. A separate set of cells were tested for each selected drug. Stock solutions of the drugs were prepared by dissolving them in separate autoclaved Milli-Q water. The selected drugs (all purchased from Wako) and their corresponding final concentration are as follows: propranolol (0.3–30  $\mu\text{M}$ ), isoproterenol (0.01–1  $\mu\text{M}$ ), quinidine (2–200  $\mu\text{M}$ ), verapamil (0.01–1  $\mu\text{M}$ ), sotalolol (1–100  $\mu\text{M}$ ), and acetylsalicylic acid (0.1–10  $\mu\text{M}$ ).

### Simultaneous recording of field potential and contractile motion of cells exposed to verapamil

The same cell plating and the drug administration protocols discussed in the previous sections were performed in MEA probes (MED-P515A, Alpha MED Sciences, Osaka, Japan) but the total culture media was reduced to 2 mL. Synchronized

acquisition of the video recording and the multi-electrode array (MEA) recording were controlled by the MEA system. Sampling frequency of 20 kHz and bandwidth of 1-1000 Hz were set for the 64 electrodes that were analysed by Mobius Software (Alpha MED Sciences) to detect and average ( $n=10$ ) the field potential duration; similar to previous reports.<sup>28,33</sup>

## Results and discussion

### Effects of drugs on the beating rate of mESC-CMs

The pharmacological responses of mESC-CMs were investigated from the observed beating cells. Beating mESC-CMs were generally observed 12 days after placing the EBs on the gelatine-coated wells; 17 days including culturing in hanging drop method.

Fig. 3 illustrates how the pharmacological effect profiles of the drugs were generated. A 650 ms mean beat interval of mESC-CMs was increased to 705 ms after 1 min exposure to 0.01  $\mu\text{M}$  verapamil; indicating a decrease in beat rate (Fig. 3a) and a change ratio (%) of -8.46%. Increasing the concentration of verapamil to 0.1  $\mu\text{M}$  (Fig. 3b) and 1  $\mu\text{M}$  (Fig. 3c) result to a change ratio of -40% and -95%, respectively. The summary of the responses is presented into a graph (Fig. 3d).

Verapamil blocks L-type  $\text{Ca}^{2+}$  channels which, in effect, decreases the cytoplasmic  $\text{Ca}^{2+}$  concentration associated with the  $\text{Ca}^{2+}$  induce and release mechanism manifested by the contraction-relaxation motion.<sup>28</sup> This explains the progressive increase in beat interval with increased verapamil concentration. This inhibition is expected to be concentration-dependent that is similar to other reports.<sup>28,34,35</sup>

A similar approach was done with the remaining drugs and the result is summarized in Fig. 4. Acetylsalicylic acid or aspirin was used as negative control because of its low to no myocardial performance. A less than 10% change ratio was observed from mESC-CMs exposed with 0.1–10  $\mu\text{M}$  of acetylsalicylic acid (Fig. 4 Acetylsalicylic acid). This demonstrated that the solvent used in the experiment has little to no effect with the beat behaviour of the cell.

In the presence of isoproterenol, known as a  $\beta$ -adrenoceptor agonist, the change ratio increased by ~50% at 1  $\mu\text{M}$ ; illustrating the expected increase in beat rate which is conventionally measured by electrophysiological method.<sup>36–38</sup> However, this positive chronotropic effect was not seen when exposed with 0.01  $\mu\text{M}$  of isoproterenol (Fig. 4 Isoproterenol). This indicates that at this low concentration, the amount of activated  $\beta$ -receptors was not enough to significantly alter the motion of the cells. It is important to note that a progressive increase in change ratio was observed after increasing the concentration of isoproterenol from 0.01  $\mu\text{M}$ .

Aside from verapamil as a negative chronotropic agent, quinidine ( $\text{Na}^+$  channel blocker), propranolol ( $\beta$  and  $\text{Na}^+$  channel blocker), and sotalol ( $\beta$  and  $\text{K}^+$  channel blocker) were administered to mESC-CMs. Different modes of action are associated to each drug but all are known to decrease the beat rate. Based on Fig. 4 the agents can be ranked according to the

least concentration needed for a significant decrease in beat rate. Verapamil ranked first followed by propranolol, quinidine, and sotalol in order. Altering the  $\text{Ca}^{2+}$  concentration in the cells has, therefore, the greatest chronotropic effect. This is expected since  $\text{Ca}^{2+}$  release from the sarcoplasmic reticulum, which underlies cardiac contraction in general is triggered and coordinated with the entry of  $\text{Ca}^{2+}$  from the cytoplasm.<sup>39</sup>

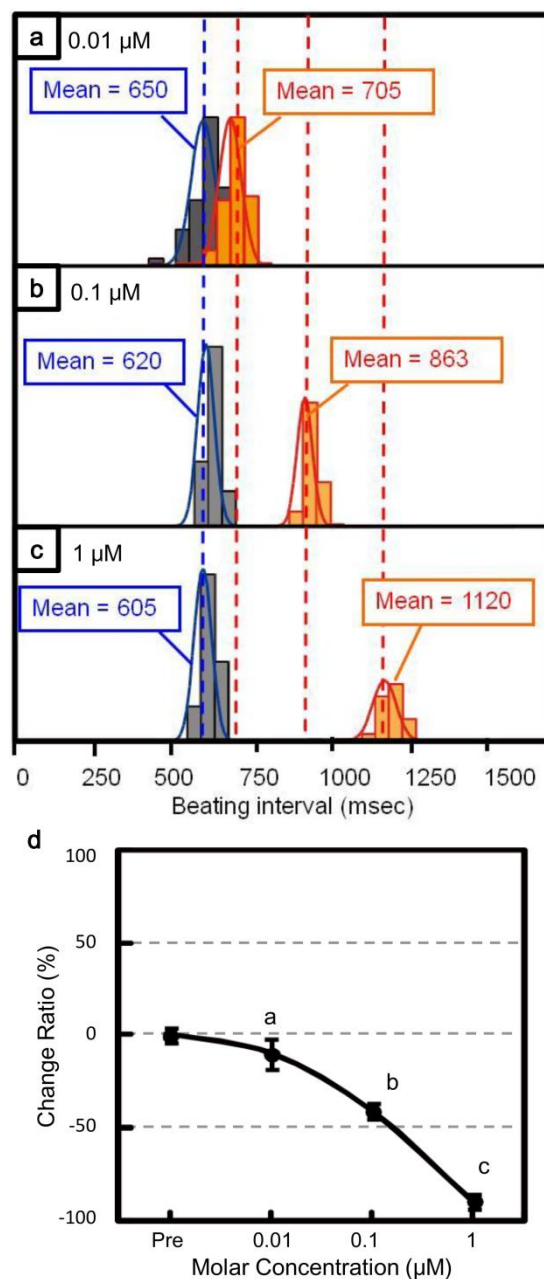


**Fig. 3.** Pharmacological effect profile generation. Verapamil was exposed to beating mESC-CMs at different concentrations: (a) 0.01  $\mu\text{M}$ , (b) 0.1  $\mu\text{M}$ , and (c) 1  $\mu\text{M}$ . The comparison of the mean beat intervals produced by Gaussian fitting on the histograms of before (blue font) and after (red font) drug administration was the key parameter for the profile. (d) Produced chronotropic effect profile of verapamil based on the change ratio of the beat intervals at different molar concentration. Change ratio (%) =  $100 \times (\text{beat interval before administration} - \text{beat interval after administration}) / \text{beat interval before administration}$ . Error bar represents the standard deviation of the mean (n = 10).

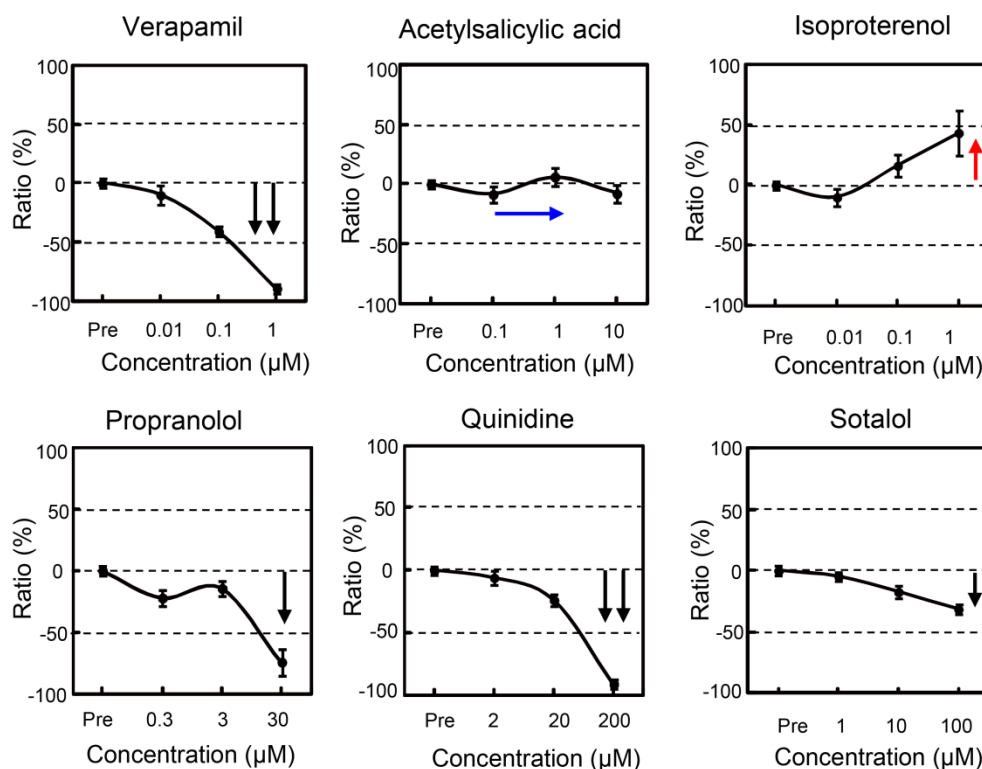


Fig. 4. Pharmacological responses of mESC-CMs on selected drugs quantified by the imaging analysis. Horizontal axis corresponds to the final concentration of the drug while the vertical axis corresponds to the calculated change ratio; change ratio (%) =  $100 \times (\text{beat interval before administration} - \text{beat interval after administration}) / \text{beat interval before administration}$ . Chronotropic effect of the drugs can be easily inferred from the graphs. Isoproterenol is a positive chronotropic agent while acetylsalicylic acid does not alter the beat rate significantly. Among the negative chronotropic agents, verapamil is the most potent (~100% at 1  $\mu\text{M}$ ) followed by propranolol, quinidine, and sotalol. Error bar represents the standard deviation of the mean (n=3).

Quinidine, as  $\text{Na}^+$  channel blocker, affects the inward  $\text{Na}^+$  flux and depolarization phase of cardiac action potential which delays the activation of  $\text{K}^+$  channels and  $\text{Ca}^{2+}$  channels. It prolongs the cardiac potential and subsequently prolongs the beat interval. Fig. 4 shows that 200  $\mu\text{M}$  of quinidine, which is ~200x higher than verapamil, was required for a change ratio of ~ -100%.

Propranolol is a widely-used non-selective  $\beta$ -adrenergic receptor antagonist that is discovered to block  $\text{Na}^+$  channels.<sup>40</sup> As a  $\beta$ -adrenergic receptor blocker, it prevents the ligands to bind and, in effect, the G-protein complex associated with the receptor cannot activate the production of cyclic adenosine monophosphate which is responsible for turning on the

calcium inflow channels and, thus, decrease the beat rate.<sup>41, 42</sup> Adding this to  $\text{Na}^+$  channel blocking effect, this explains the -86% change ratio at 30  $\mu\text{M}$  of propranolol which is more potent than quinidine as a negative chronotropic agent (Fig. 4). However, concentration-dependent inhibition was not observed at a concentration below 3  $\mu\text{M}$  which may indicate a different drug pathway mechanism which is beyond the scope of this report.

Another non-selective  $\beta$ -adrenergic receptor blocker agent administered was sotalol, that has  $\text{K}^+$  channel blocking ability. Aside from  $\beta$ -adrenergic receptor blocking, a decrease in beat rate is due to the prolong repolarization phase of the cardiac potential and delay in relaxation of the cell. Concentration-

Drugs	Class	Result	Clinical Efficacy
		Beat Frequency	Beat Frequency
Acetylsalicylic acid	-	→ (0% @ 10 $\mu\text{M}$ )	→
Isoproterenol	$\beta$ stimulant	↑ (50% @ 1 $\mu\text{M}$ )	↑
Verapamil	$\text{Ca}^{2+}$ channel blocker	↓↓ (-100% @ 1 $\mu\text{M}$ )	↓↓
Propranolol	$\beta$ and $\text{Na}^+$ channel blocker	↓↓ (-86% @ 30 $\mu\text{M}$ )	↓↓
Quinidine	$\text{Na}^+$ channel blocker	↓↓ (-100% @ 200 $\mu\text{M}$ )	↓↓
Sotalol	$\beta$ and $\text{K}^+$ channel blocker	↓ (-45% @ 100 $\mu\text{M}$ )	↓

Table 1. Comparison of the chronotropic effects of the drugs and their known clinical empirical result.

dependent inhibition was observed but at 100  $\mu\text{M}$ , it only has a change ratio of  $\sim 45\%$ . Sotalol binds to channels better at slower rates of activation and are more potent at slower beat rates.<sup>43</sup> Thus at a normal or higher beat rate, this is the least potent among the negative chronotropic drugs administered which is reflected in Fig. 4.

A summary of the empirical result of the drugs administered in comparison to their known chronotropic effect is presented in Table 1. This result shows the applicability of the method to quantitatively profile the administered drugs. In addition, this analytical method made it possible to quantify the beat rate at any place where differentiated EB is located, which cannot be achieved by conventional electrophysiological method.

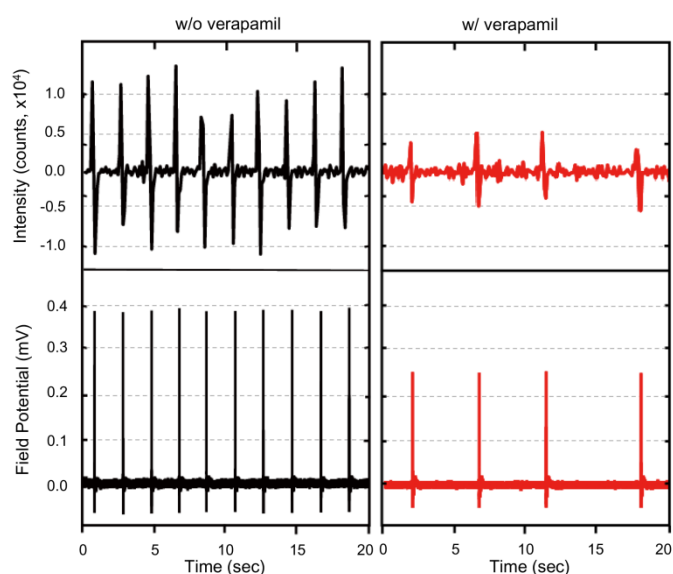


**Fig. 5.** Simultaneous measurement of field potential and contractile motion before and after exposure to verapamil (1  $\mu\text{M}$ ). First row shows the derivative imaging analysis while the second row shows MED analysis of the monitored beating of mESC-CMs. Comparison of the readings before (first column) and after (second column) verapamil administration shows coherent signal generation. As expected, a decrease in beat rate can be observed from the graphs. In addition, the profile generated from the derivative imaging analysis shows that the contraction-relaxation motion relatively became uniform after administration of verapamil, which is not reflected in the MED analysis.

### Comparison of field potential to contractile data

For comparison, the field potential was measured with MEA simultaneously with the video recording of the contractile motion of the observed cells. The first column in Fig. 5 shows the contractile profile and field potential profile of the beating mESC-CM before verapamil (1  $\mu\text{M}$ ) administration while the second column is for after 1 min of administration. It can be observed that the occurrence and interval of the beats were coherent in both methods. Before administration, the systolic or contraction process, represented in the upstroke signal in the field potential, was uniform throughout the recording (max at  $\sim 0.4$  mV). In contrast, the systolic process, represented by the positive amplitudes of the beat motion, was fluctuated.

This indicates that the movement of the cardiomyocytes was not uniform for each beat which cannot be reflected in the profile from MEA. In addition, the diastolic or relaxation process, which was undetectable in MEA measurement, was fluctuated in each beat as seen in the contractile motion profile. The electrophysiological and morphological observations were more distinguished after verapamil administration (Fig. 5). Since verapamil is a  $\text{Ca}^{2+}$  blocker, the action potential and, subsequently, the physical movement of the cardiomyocyte will be reduced. Comparing the change in the measured field potential to the change in measured intensity counts, both had a  $\sim 50\%$  decrease. This indicates the possible use of this method to quantify the  $\text{Ca}^{2+}$  present which is similar to some reports.<sup>28,34</sup> In addition, after administration of verapamil, the contractile motion profile showed that the diastolic process was about the same as that in the systolic process; indicating a uniform contraction-relaxation motion. This is also not reflected in the field potential measurement. Therefore, aside from generating the same beat occurrence, the profile generated with the microscopic imaging system provided more information than the profile generated by the MEA.

### Conclusions

The imaging analysis used to generate the contractile motion profile of the beating mESC-CMs using a microscope camera operated at a low setting has been demonstrated in evaluating the chronotropic effects of six selected drugs. As a cheap, non-invasive, and label-free tool, continuous monitoring can be done on the cells as an extension of the study which can provide insights on *in vivo* pathophysiology in the cells. In addition, the signal from the contractile motion profile was coherent with the field potential profile that can be measured regardless of cell location. With these findings, it is expected that this approach can be helpful to *in vitro* profiling of compound entities in pre-clinical drug discovery and development for the pharmaceutical and medical industry.

### Acknowledgements

Yoshinori Yamaguchi would like to acknowledge, partly, the Grand-in-Aid for Scientific Research (Houga) for the financial support. (No. 25600049(Y.Y.), JSPS, Japan.

### References

- 1 V. Ahuja and S. Sharma, *J. Appl. Toxicol.*, 2014, **34**, 576–94.
- 2 B. Xi, N. Yu, X. Wang, X. Xu and Y. A. Abassi, *Biotechnol. J.*, 2008, **3**, 484–495.
- 3 H. G. Laverty, C. Benson, E. J. Cartwright, M. J. Cross, J. Garland, T. Hammond, C. Holloway, N. McMahon, J. Milligan, B. K. Park, M. Pirmohamed, C. Pollard, J. Radford, N. Room, P. Sager, S. Singh, T. Suter, W. Suter, A. Trafford, P. G. Volders, R. Wallis, R. Weaver, M. York and J. P. Valentin, *Br. J. Pharmacol.*, 2011, **163**, 675–693.

- 1  
2  
3  
4  
5  
6  
7  
8  
9  
10  
11  
12  
13  
14  
15  
16  
17  
18  
19  
20  
21  
22  
23  
24  
25  
26  
27  
28  
29  
30  
31  
32  
33  
34  
35  
36  
37  
38  
39  
40  
41  
42  
43  
44  
45  
46  
47  
48  
49  
50  
51  
52  
53  
54  
55  
56  
57  
58  
59  
60
- 4 M. Liu, Y. Wu, Y. Chen, J. Sun, Z. Zhao, X. -W. Chen, M. E. Matheny and H. Xu, *J. Am. Med. Informatics Assoc.*, 2012, **19**, e28–e35.
- 5 I. Itzhaki, L. Maizels, I. Huber, L. Zwi-Dantsis, O. Caspi, A. Winterstern, O. Feldman, A. Gepstein, G. Arbel, H. Hammerman, M. Boulos and L. Gepstein, *Nature*, 2011, **471**, 225–229.
- 6 T. Tanaka, S. Tohyama, M. Murata, F. Nomura, T. Kaneko, H. Chen, F. Hattori, T. Egashira, T. Seki, Y. Ohno, U. Koshimizu, S. Yuasa, S. Ogawa, S. Yamanaka, K. Yasuda and K. Fukuda, *Biochem. Biophys. Res. Commun.*, 2009, **385**, 497–502.
- 7 C. Denning and D. Anderson, *Drug Discov. Today Ther. Strateg.*, 2008, **5**, 223–232.
- 8 T. Meyer, P. Sartipy, F. Blind, C. Leisgen and E. Guenther, *Expert Opin. Drug Metab. Toxicol.*, 2007, **3**, 507–517.
- 9 K. Musunuru, I. J. Domian and K. R. Chien, *Annu. Rev. Cell Dev. Biol.*, 2010, **26**, 667–687.
- 10 J. R. Plews, M. Gu, M. T. Longaker and J. C. Wu, *J. Cell. Mol. Med.*, 2012, **16**, 1196–1202.
- 11 N. Sun, M. Yazawa, J. Liu, L. Han, V. Sanchez-Freire, O. J. Abilez, E. G. Navarrete, S. Hu, L. Wang, A. Lee, A. Pavlovic, S. Lin, R. Chen, R. J. Hajjar, M. P. Snyder, R. E. Dolmetsch, M. J. Butte, E. A. Ashley, M. T. Longaker, R. C. Robbins and J. C. Wu, *Sci. Transl. Med.*, 2012, **4**, 130ra47–130ra47.
- 12 J. W. A. Ebert, P. Liang, *J. Cardiovasc. Pharmacol.*, 2012, **60**, 408–416.
- 13 N. Yokoo, S. Baba, S. Kaichi, A. Niwa, T. Mima, H. Doi, S. Yamanaka, T. Nakahata and T. Heike, *Biochem. Biophys. Res. Commun.*, 2009, **387**, 482–488.
- 14 A. M. Wobus, G. Kaomei, J. Shan, M. C. Wellner, J. Rohwedel, Ji Guanju, B. Fleischmann, H. A. Katus, J. Hescheler and W. M. Franz, *J. Mol. Cell. Cardiol.*, 1997, **29**, 1525–1539.
- 15 S. Stoelzle, A. Haythornthwaite, R. Kettenhofen, E. Kolossov, H. Bohlen, M. George, A. Brüggemann and N. Fertig, *J. Biomol. Screen. Off. J. Soc. Biomol. Screen.*, 2011, **16**, 910–916.
- 16 A. Stett, U. Egert, E. Guenther, F. Hofmann, T. Meyer, W. Nisch and H. Haemmerle, *Anal. Bioanal. Chem.*, 2003, **377**, 486–495.
- 17 H. Liang, M. Matzkies, H. Schunkert, M. Tang, H. Bonnemeier, J. Hescheler and M. Reppel, *Cell. Physiol. Biochem.*, 2010, **25**, 459–466.
- 18 J.-Q. He, Y. Ma, Y. Lee, J. A. Thomson and T. J. Kamp, *Circ. Res.*, 2003, **93**, 32–39.
- 19 C. Mauritz, K. Schwanke, M. Reppel, S. Neef, K. Katsirntaki, L. S. Maier, F. Nguemo, S. Menke, M. Haustein, J. Hescheler, G. Hasenfuss and U. Martin, *Circulation*, 2008, **118**, 507–517.
- 20 P. Sasse, J. Zhang, L. Cleemann, M. Morad, J. Hescheler and B. K. Fleischmann, *J. Gen. Physiol.*, 2007, **130**, 133–144.
- 21 J. S. Leyton-Mange, R. W. Mills, V. S. Macri, M. Y. Jang, F. N. Butte, P. T. Ellinor and D. J. Milan, *Stem Cell Reports*, 2014, **2**, 163–170.
- 22 J. Gorelik, N. N. Ali, A. I. Shevchuk, M. Lab, C. Williamson, S. E. Harding and Y. E. Korchev, *Tissue Eng.*, 2006, **12**, 657–664.
- 23 J. Gorelik, N. N. Ali, S. H. Sheikh Abdul Kadir, M. Lab, P. Stojkovic, L. Armstrong, E. V. Sviderskaya, Y. A. Negulyaev, D. Klenerman, D. C. Bennett, M. Lako, S. E. Harding, M. Stojkovic and Y. E. Korchev, *Tissue Eng. Part C. Methods*, 2008, **14**, 311–318.
- 24 Q. Liu, H. Yu, Z. Tan, H. Cai, W. Ye, M. Zhang and P. Wang, *Sensors Actuators, B Chem.*, 2011, **155**, 214–219.
- 25 G. Vescovo, S. E. Harding, S. M. Jones, L. Dalla Libera, A. C. Pessina and P. A. Poole-Wilson, *Basic Res. Cardiol.*, 1989, **84**, 536–543.
- 26 S. E. Harding, G. Vescovo, M. Kirby, S. M. Jones, J. Gurden, B. Street and W. I. N. London, *J. Mol. Cell. Cardiol.*, 1988, **20**, 635–647.
- 27 B. W. Steadman, K. B. Moore, K. W. Spitzer and J. H. B. Bridge, *IEEE Trans. Biomed. Eng.*, 1988, **35**, 264–272.
- 28 T. Hayakawa, T. Kunihiro, T. Ando, S. Kobayashi, E. Matsui, H. Yada, Y. Kanda, J. Kurokawa and T. Furukawa, *J. Mol. Cell. Cardiol.*, 2014, **77**, 178–191.
- 29 T. Hayakawa, T. Kunihiro, S. Dowaki, H. Uno, E. Matsui, M. Uchida, S. Kobayashi, A. Yasuda, T. Shimizu and T. Okano, *Tissue Eng. Part C Methods*, 2012, **18**, 21–32.
- 30 A. Ahola, A. L. Kiviahio, K. Larsson, M. Honkanen, K. Aaito-Setälä and J. Hyttinen, *Biomed. Eng. Online*, 2014, **13**, 39.
- 31 M. M. Hossain, E. Shimizu, M. Saito, S. R. Rao, Y. Yamaguchi and E. Tamiya, *Analyst*, 2010, **135**, 1624–1630.
- 32 W. Espulgar, Y. Yamaguchi, W. Aoki, D. Mita, M. Saito, J.-L. Lee and E. Tamiya, *Sensors Actuators B Chem.*, 2015, **207**, 43–50.
- 33 K. Yamazaki, T. Hihara, T. Taniguchi, N. Kohmura, Y. Yoshinaga, M. Ito and K. Sawada, *Toxicol. Vitro.*, 2012, **26**, 335–342.
- 34 T. Wang, N. Hu, J. Cao, J. Wu, K. Su and P. Wang, *Biosens. Bioelectron.*, 2013, **49**, 9–13.
- 35 H. M. Himmel, *J. Pharmacol. Toxicol. Methods*, 2013, **68**, 97–111.
- 36 K. Guan, S. Wagner, B. Unsöld, L. S. Maier, D. Kaiser, S. Hemmerlein, K. Nayernia, W. Engel and G. Hasenfuss, *Circ. Res.*, 2007, **100**, 1615–1625.
- 37 J. Hescheler, M. Halbach, U. Egert, Z. J. Lu, H. Bohlen, B. K. Fleischmann and M. Reppel, in *J. Electrocardiol.*, 2004, **33**, 110–116.
- 38 H. Baharvand, A. Piryaeei, R. Rohani, A. Taei, M. H. Heidari and A. Hosseini, *Cell Biol. Int.*, 2006, **30**, 800–807.
- 39 V. Lukyanenko, A. Chikando and W. J. Lederer, *Int. J. Biochem. Cell Biol.*, 2009, **41**, 1957–1971.
- 40 D. W. Wang, A. M. Mistry, K. M. Kahlig, J. A. Kearney, J. Xiang and A. L. George, *Front. Pharmacol.*, 2010, **DEC**, 1–12.
- 41 L. Bertrix, Q. Timour-Chah, J. Lang, M. Lakhal and G. Faucou, *Cardiovasc. Res.*, 1986, **20**, 358–363.
- 42 A. L. Waldo, A. J. Camm, H. DeRuyter, P. L. Friedman, D. MacNeil, J. F. Pauls, B. Pitt, C. M. Pratt, P. J. Schwartz and E. P. Veltri, *Lancet*, 1996, **348**, 7–12.
- 43 M. Razavi, *Tex. Heart Inst. J.*, 2005, **32**, 209–211.